Analysis of 3GM High Accuracy Accelerometer data collected during JUICE Lunar Earth Gravity Assist

Authors: Umberto De Filippis [1*], Paolo Cappuccio[2], Mauro Di Benedetto [1], Ivan di Stefano [1], Daniele Durante [1], Luciano Iess[1]

[1*]Sapienza University of Rome, 00184 Rome, Italy
[1]Sapienza University of Rome, 00184 Rome, Italy
[2]Aurora Technology BV for ESA, European Space Agency, European Space Astronomy Centre (ESAC), Camino Bajo del Castillo s/n, Villanueva de la Canada, 28692, Madrid, Spain

Correspondence to: Umberto De Filippis, umberto.defilippis@ext.esa.int

Abstract

The JUpiter ICy moons Explorer (JUICE) mission, launched in April 2023 by the European Space Agency (ESA), is designed to investigate Jupiter and its largest icy moons, Ganymede, Callisto, and Europa, with a focus on assessing their potential habitability and investigating subsurface oceans. During its eight-year interplanetary cruise to the Jovian system, JUICE is scheduled to perform several flybys. The first of these, the combined Lunar-Earth Gravity Assist (LEGA), took place in August 2024.The spacecraft is equipped with a High Accuracy Accelerometer (HAA) that is part of the Gravity and Geophysics of Jupiter and the Galilean Moons (3GM) radio science instrument. During LEGA operations, HAA collected two hours of scientific data centered across the Moon's closest approach. We present here a detailed analysis of the HAA calibrated measurements that show a strong agreement with predicted non-gravitational accelerations, including those related to spacecraft deformation caused by the Moon's gravity gradient and thermoelastic displacements of the solar arrays during penumbra transitions. Additionally, unexpected dynamic responses were observed, including structural vibrations excited by the movement of the steerable telescope of the Submilimetre Wave Instrument (SWI) and a distinct outgassing event detected shortly after crossing the lunar terminator. The outgassing, likely involving sublimated water ice on the spacecraft, resulted in a measurable velocity change of 0.7 ± 0.1 mm/s along the -Z spacecraft axis and a consequent mass loss of a few grams. This direction coincides with the normal direction of the spacecraft's most exposed surface to the Moon illuminated surface. The JUICE orbital reconstruction derived from radio tracking data collected by the Deep Space Transponder (DST) confirmed a consistent velocity variation, supporting HAA findings. These in-flight observations are essential for instrument calibration, characterization of the spacecraft's dynamic environment, and refining operational strategies.

1 Introduction

The JUpiter ICy moons Explorer (JUICE) is an ESA large class mission launched on April 14, 2023 Grasset *et al.,* (2013). It represents a significant opportunity to explore the Jovian system using a state-of-the-art suite of instruments. Focusing on Jupiter and its three largest icy moons, Ganymede, Callisto, and Europa, the mission's primary objective is to investigate the moons' potential habitability and the likely presence of subsurface oceans, which may harbor conditions suitable for life.

The 8-year interplanetary cruise includes 3 Earth flybys and 1 Venus flyby, crucial for a timely arrival at Jupiter. The first Earth encounter after the launch was a lunar-Earth gravity assist (LEGA), occurred on August 19-20, 2024, and being the first-ever double gravity assist of human history in space exploration. This critical maneuver was essential for redirecting JUICE towards Venus, where another gravity assist occurred in August 2025. Subsequent flybys of the Earth in 2026 and 2029 will further refine the spacecraft's path, ensuring it will reach Jupiter with the correct speed and direction. These flybys are not merely navigational aids but also opportunities for scientific observations. These data could indeed contribute to refine our understanding of these bodies and support the calibration of JUICE's instruments.

Upon arrival at Jupiter in July 2031, JUICE will start its detailed exploration of the Jovian system, culminating in an extended circular polar and low altitude orbit phase around Ganymede. The orbital phase will provide unprecedented insights into the moons' geology, extent of the subsurface ocean, and potential habitability, significantly advancing our knowledge of the outer Solar System, Grasset et al., (2023).

The High Accuracy Accelerometer (HAA) is one of the instrument onboard JUICE and its main goal is to support the Gravity and Geophysics of Jupiter and the Galilean Moons (3GM) radio science experiment. The accelerometer data will be used within the orbit determination process as a direct measurement of the non-gravitational perturbations acting on the spacecraft, particularly those due to the propellant sloshing. From the very early stages of the mission, HAA data played a crucial role in monitoring the spacecraft's deployable components. Within the first six weeks following JUICE's launch, the Mission Operation Control (MOC) team successfully deployed solar panels, antennas, probes, and booms that had been folded and latched during launch. The data collected by HAA offered valuable insights into the spacecraft's dynamics and a monitoring of the deployment operations, De Filippis et al., (2024).

During LEGA operations, HAA was switched ON in observation mode and collected data for two hours across the Moon closest approach (CA), providing direct measurements of the spacecraft's dynamics response to the solar eclipse, Moon gravity gradient and additional non gravitational perturbations acting on the probe.

The paper is organized as follows. In the following two sections the 3GM experiment and the HAA instrument are described. The third section deals with the LEGA geometry and HAA operations timeline. In the same section are discussed the expected and unexpected signals detected by HAA along with the instrument data analysis and interpretation. The last section contains conclusions.

2 The 3GM experiment

The 3GM instrument suite is devoted to radio science experiments, whose goals can be grouped in two main areas: geodesy and geophysics for Callisto, Europa and Ganymede, and atmospheric science of Jupiter. Gravity experiments will be performed using the Ka band two-way coherent radio link, enabled by the Ka band Transponder (KaT). Thanks to this state-of-art instrument, developed by Thales Alenia Space Italy, two-way range and Doppler observables can achieve a precision, respectively, of 4 cm at 10 s integration time (depending of the available signal to noise ratio) and of 3 μm/s at 1000 s integration time Cappuccio et al., (2018); Cappuccio et al., (2020). The occultation experiments will use the onboard ultra stable oscillator (USO), built by AccuBeat, to perform accurate one-way radio occultations. The USO can generate onboard a highly stable 57.5 MHz reference signal with an Allan deviation of about $1 - 2 \times 10^{-13}$ over a broad range of integration times [1–1000 s], A. Shapira et al., (2016).

A previous analysis has shown that thanks to the Callisto's flybys, 3GM experiment will be capable to determine its gravity field up to degree and order 7 and improve notably the accuracy on the determination of the love number k_2 ($\sigma_{k_2} \leq 0.06$). The two close encounters of JUICE with Europa will allow 3GM to improve the knowledge of the quadrupole gravity field and verify the hydrostatic equilibrium hypothesis at the level of 0.5%, Cappuccio *et al.,* (2022) .
However, the main objective of the JUICE mission is to perform a full tomography of Ganymede, thanks to the combination of 3GM observations with other instruments data.
Previous simulations showed that the moon's gravity field can be confidently determined up to degree 35–40, together with a detailed characterization of the rotational state and tides; Cappuccio *et al.*,(2020); De Marchi et al., (2022).
Furthermore, three superior solar conjunctions occurring during the cruise phase provide opportunities for the 3GM radio science experiment to perform tests of general relativity, di Stefano et al., (2022).
These scientific goals can be reached only if a very accurate dynamical model is used for the numerical integration of the spacecraft trajectory. Given the spacecraft structure, previous simulations showed that accelerations due to sloshing within the fuel tanks could severely affect the expected radio science outcome, Cappuccio et al., (2018). For this reason, 3GM will also exploit data collected by the on-board High Accuracy Accelerometer (HAA) to calibrate non-gravitational perturbations.

3 The High Accuracy Accelerometer

The High Accuracy Accelerometer is the second spring mass accelerometer ever flown on an interplanetary spacecraft. The instrument is built on the heritage of the Italian Spring Accelerometer (ISA) which is currently flying on BepiColombo ESA/JAXA mission, Benkhoff et al., (2021). ISA has been developed by the Gruppo di Gravitazione Sperimentale at the Institute for Space Astrophysics and Planetology (INAF-IAPS) whereas Thales Alenia Space Italy is the manufacturer of both the HAA and ISA instruments [13] Santoli *et al.*, (2020). ISA data in the BepiColombo mission have been used so far to better understand the spacecraft dynamics during flybys, Magnafico *et al.,(2025)*, Del Vecchio et al., (2025) and will be used within the orbit determination software to enhance the reliability of the Mercury Orbiter Radio science Experiment (MORE) results, De Filippis *et al., (2024)*.

The HAA consists of two units: the Accelerometer Control Unit (ACU) and the Accelerometer Detector Assembly (ADA). The ADA hosts three sensors with their relevant element being a very thin slat. The sensing mass works as a mechanical harmonic oscillator with a resonance frequency of about 3.6 Hz. To reduce the down-conversion of out-of-band high-frequency signals, the HAA is equipped with an out-of-band mechanical noise rejection algorithm. This algorithm makes use of a polynomial filter which linearizes the instrument characteristic response. The coefficients of the polynomial function can be found by applying a square wave with the actuators when the disturbance is acting.

Comparing the reading of each accelerometer sensor with the expected output, it's possible to find the coefficients with a simple least square estimation.

The accelerations are detected by measuring the movements of the proof mass within the instrument's frame. These movements are converted into voltage signals by pick-up capacitors. The three sensors, indicated as Acc0, Acc1 and Acc2, are mounted on mechanical dampers over the electronic module, which contains the Front-End Electronic (FEE) board. The ACU interfaces with the spacecraft and controls the ADA assembly. The HAA software provides four independent thermal controls, one for each sensor and one for the FEE. The temperature-controlled point is located on the ADA box. The instrument inflight calibration is conducted using a couple of control capacitors which are placed under the pick-up capacitors. These capacitors can be seen as actuators which are able to apply a reference signal to the proof mass. Table 1 shows the instrument performance indexes declared by the manufacturer after ground tests.

Performance index	**Value**
Measurement bandwidth	$[10^{-4} – 10^{-1}]$ Hz
Measurement accuracy	10^{-8} m/s^2
Electronic thermal sensitivity	10^{-8} m/s^2/°C
Intrinsic thermal sensitivity	5×10^{-7} m/s^2/°C
Thermal control attenuation factor	700
Intrinsic noise floor	10^{-9} m/s^2/ $\sqrt{Hz}$
Scale factor accuracy	1%

Table 1 HAA performance indexes

The expected measurement accuracy depends on frequency. Its spectral density is constant at $8 \times 10^{-9} \frac{m}{s\sqrt{Hz}}$ over the frequency range $[10^{-1}, 7 \times 10^{-4}]$ Hz, and increases linearly to $3 \times 10^{-8} \frac{m}{s\sqrt{Hz}}$ over the range $[7 \times 10^{-4}, 10^{-4}]$ Hz.

In-flight instrument performance will be assessed after the thermal control optimization will be completed.

4 Lunar-Earth gravity assist

The JUICE mission employs a sequence of gravity assists to increase its energy and adjust its trajectory for the long journey to the Jovian system. Among these, the Lunar-Earth Gravity Assist (LEGA), performed in August 2024, represents a novel and highly efficient maneuver. By first performing a flyby of the Moon with CA at 750 km, followed just few hours later by an Earth flyby (CA at 6800 km), JUICE exploited the combined gravitational influence of both bodies to achieve a substantial change in its heliocentric velocity. This dual-body gravity assist allowed to significantly reduce propellant consumption, enabling the spacecraft to reorient its path toward subsequent Venus and Earth flybys.

4.1 HAA operations

The onboard accelerometer was switched ON two days before the lunar gravity assist to ensure the instrument reached passive thermal stabilization. Although both the sensors and the FEE are equipped with active thermal control systems, these were not activated during LEGA operations, because analyses of other in-flight data acquired during earlier instrument checkouts highlighted the need to still optimize the thermal control settings.

The instrument started to collect data ~ 1 hours before Moon CA after a self-calibration and remained in observation mode until 1 hour after Moon CA. Fig. 1 shows the timeline of HAA operations. In this time window, different phenomena were expected to produce dynamical effects on the spacecraft, raising the interest to switch on the instrument.

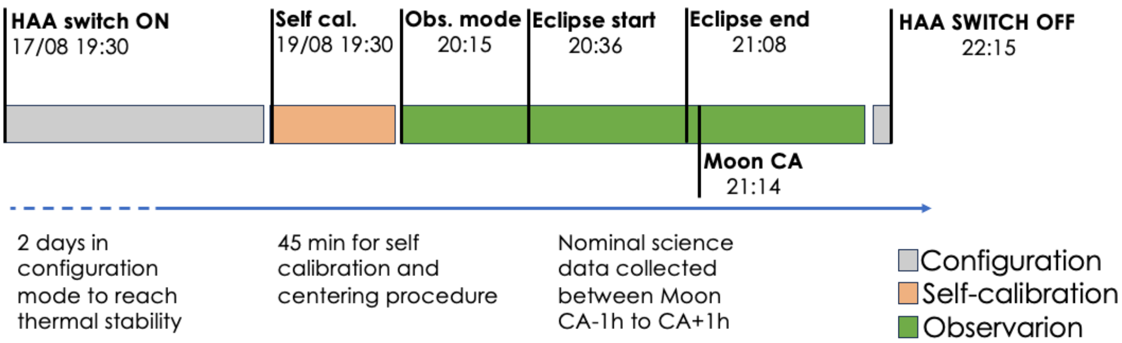

Fig. 1 HAA operations during Lunar gravity assist

4.2 Spacecraft attitude and expected signals

An accurate representation of the spacecraft's attitude is essential to reliably model the non-conservative forces acting on it. The latest release of the JUICE SPICE kernels, Lopez et al. (2023), has been used to retrieve the measured attitude of the spacecraft. To describe the orientation of JUICE, a body fixed reference frame is used, defined as follows: the $+\hat{x}_{SC}$ is aligned with HGA boresight but points in the opposite direction, $+\hat{z}_{SC}$ is the spacecraft upper nadir direction where some sensitive instruments are mounted on an optical bench, and $+\hat{y}_{SC}$ axis completes the right-handed frame, with $\pm\hat{y}_{SC}$ hosting the 85 m^2 solar arrays. Fig. 2 shows the relation between each accelerometer sensing axis direction and JUICE SPACECRAFT reference frame.

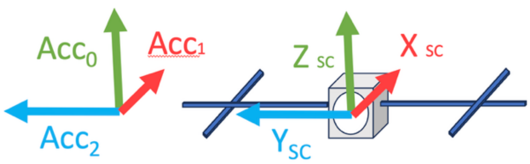

Fig. 2 HAA (left) and JUICE SPACECRAFT (right) reference frames

During the cruise phase, under nominal attitude conditions, the $-\hat{x}_{SC}$ direction axis is always oriented toward the Sun to shield the spacecraft surfaces from incoming solar heating when JUICE is below 0.89 AU away from the Sun. Temporary off-pointings (~ 1 hour) are allowed in between 0.89 and 1.34 AU, while at greater distance the HGA can point to the Earth. During the lunar flyby, the commanded spacecraft attitude was quasi-inertial, meaning that no apparent acceleration was expected to be detected by the HAA. Among all the expected signals, the Moon's gravity gradient was the most interesting one for calibration purposes and will be described in the next subsection.

4.2.1 Gravity gradient

Fig. 3 schematizes the HAA sensing elements as point masses, each associated with a sensing axis defined as the direction along which an external acceleration produces the maximum signal. Because the centers of gravity of the sensing elements do not coincide with the spacecraft's center of mass, the accelerometer is inherently sensitive to the gravity gradient generated by the Moon's gravitational field at the sensor locations. The expected signal can be computed using:

$$\boldsymbol{a}_{gg}^{i} = \frac{\mu_m}{|R_0|^3}\left(3\widehat{\boldsymbol{R}}_0\widehat{\boldsymbol{R}}_0^T - \boldsymbol{I}_{3x3}\right)\boldsymbol{r}_i \tag{1}$$

where μ_m is the Moon gravitational parameter, $\boldsymbol{R}_0$ is the position vector from JUICE center of mass to the Moon center of mass, and $\boldsymbol{r}_i$ is the position vector from JUICE center of mass to the i-*th* HAA sensing element.

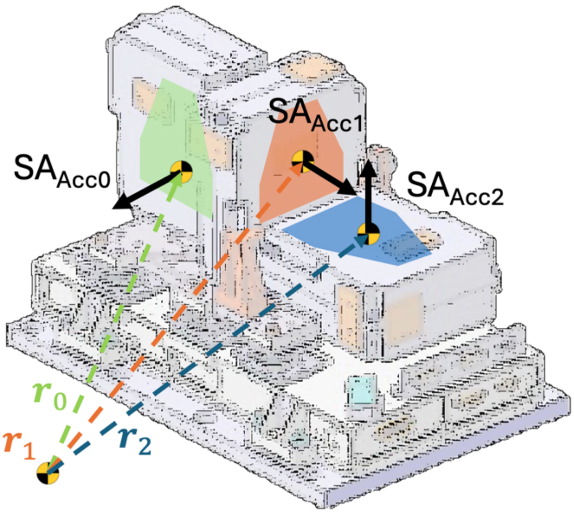

Fig. 3 HAA sensing element scheme

In this work, only data collected by the Acc0 sensor are presented, as most of the relevant signals were detected along this axis, which was also the less noisy. Fig. 4 shows the HAA calibrated data collected by the sensor Acc0 (black curve) compared with the expected gravity gradient signal (red curve). The HAA data calibration consisted of applying a low-pass filter with a cutoff frequency of

$f_c =$ 0.5 Hz to retain only frequencies within the instrument bandwidth. This was followed by a parabolic detrending procedure and a correction for thermal effects induced by temperature variations. The thermal compensation step was necessary because the instrument's thermal control system was not activated during the measurements. The correction was performed using the proof-mass thermometer readings, which were converted into equivalent acceleration signals and subsequently removed from the data. The temperature-to-acceleration conversion factor was estimated by minimizing the residuals of the calibrated acceleration after subtraction of the expected acceleration signal.

The HAA measurements show good agreement with the expected signal for most of the time, but it is evident how the black curve exhibits additional signatures, suggesting the presence of other perturbing phenomena.

The grey area corresponds to a solar eclipse experienced by the spacecraft from 20:36 UTC to 21:08 UTC, also visible in the spacecraft ground track in Fig. 5 (blue dots). The abrupt temperature change in temperature during ingress/egress phases caused thermal snaps that are described in detail in the next section.

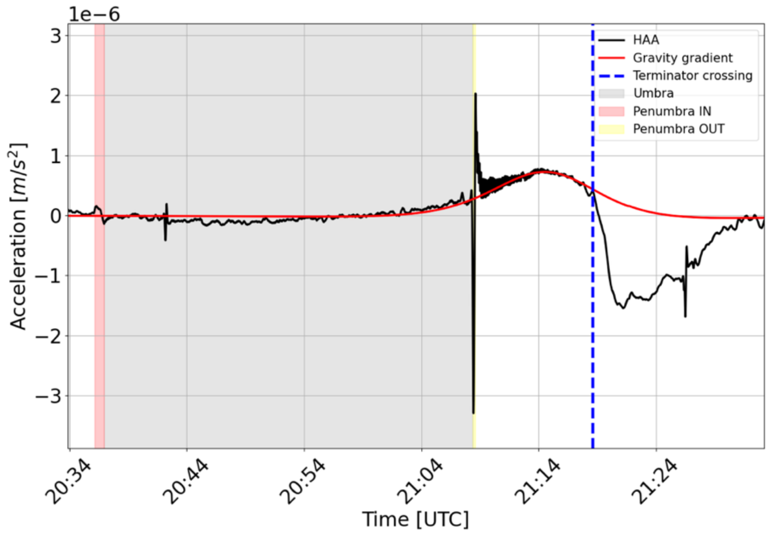

Fig. 4 HAA calibrated data collected by Acc0 sensor during LEGA. Black curve: HAA calibrated data collected by Acc0 sensor; Red curve: Expected gravity gradient signal due to the Moon; Blue dotted line: Terminator crossing event; Red and yellow shadowed areas: Ingress and egress penumbra phases; Gray shadowed area: Umbra phase

4.2.2 Thermal snap on solar array

Due to the high solar array Sun aspect angle, $\alpha \approx 70°$, the expected drop of solar radiation pressure acceleration during the eclipse was ~ 10^{-8}m/s², thus too close to the HAA measurement accuracy to be unambiguously detected. Also, the albedo pressure and infrared radiation emitted by the Moon were inducing accelerations well below the instrument's sensitivity $\sim 10^{-9}\ m/s^2$. Instead, the sudden absence of solar radiation during the eclipse caused abrupt changes in the spacecraft surface temperatures and large thermal gradient between the front and rear surfaces induced thermoelastic distortions on the structure.

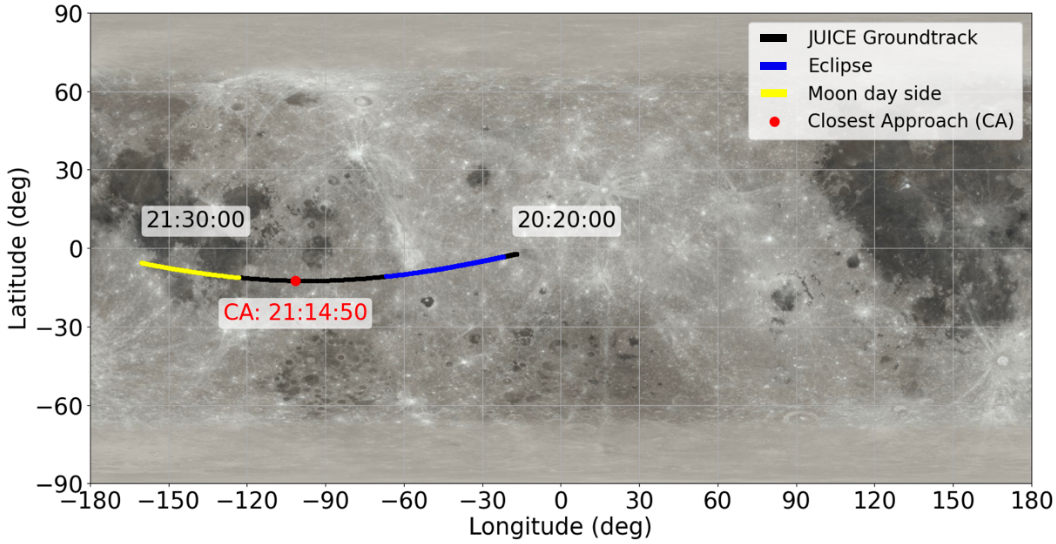

Fig. 5 JUICE ground track during Lunar gravity assist. Black curve: JUICE ground track in nightside; Yellow curve: JUICE ground track on the dayside; Blue curve: JUICE ground track during eclipse. Red dot: JUICE closest approach with Moon.

This phenomenon, known as thermal snap, can be described mathematically using (2. The resulting quasi-static displacements can be expressed in terms of the temperature difference through the thickness of the considered structure, Johnston et al. (2000). These displacements are directly proportional to both the surface thermal expansion coefficient α_{CTE} and inversely proportional the thickness h. The effect is magnified on the spacecraft solar array, due to their large surface area and small thickness, see Fig. 6. The term $(1-\nu^2)$ contains the Poisson's coefficient ν and it's used to consider the structural response of a wide plate rather than a narrow beam. If the difference between front and back surface temperatures $\Delta T = T_f - T_b$ is not constant in time, the generic point of the solar array, with a distance x from the hinge, will be subject to an acceleration $a_{ts}(t) = \frac{d^2 s_{ts}(t)}{dt^2}$ acting along the solar array normal direction $\hat{n}$, as described in (3.

$$\overrightarrow{s_{ts}}(t)|_x = -\alpha_{CTE}(1-\nu^2)\Delta T(t)\frac{x}{2h}^2\hat{n} \quad (2)$$

$$\overrightarrow{a_{ts}}(t)|_x = \frac{d^2 s_{ts}(t)}{dt^2} = -\alpha_{CTE}(1-\nu^2)\frac{d^2\Delta T(t)}{dt^2}\frac{x}{2h}^2\hat{n} \quad (3)$$

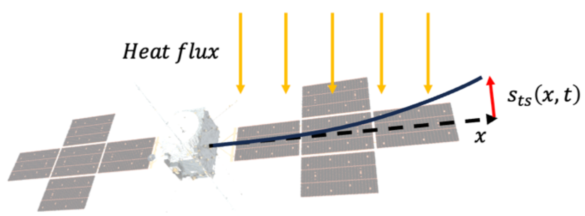

Fig. 6: JUICE solar array displacement due to thermal snap

Unfortunately, for the JUICE spacecraft only the solar array back surface temperature T_b can be retrieved from thermistors telemetry, while the front one T_f is available at a frequency of only one data point per month. For this reason, to reconstruct the ΔT curve during the eclipse we built a thermal mathematical model that describes the heat transmission from front to rear surfaces of the arrays. The solar array is modelled as a honeycomb aluminum core surrounded by two aluminum plates that exchanges heat via conduction through the core and via radiation from the plates towards internal surfaces and to the outer space. The front temperature can be estimated by solving the following system of equations, J. and S. D. Van der Ha, (2010):

$$\begin{cases} Q_{SUN}/A_p - Q_{APR}/A_p - \sigma_{SB}\varepsilon_{SA,f}T_f^4 - \dfrac{kA_{al}}{h}\left(T_f - T_b\right) - \sigma_{SB}\dfrac{\varepsilon_i(1-A_{al})}{2-\varepsilon_i}\left(T_f^4 - T_b^4\right) = C_{p,f}\dfrac{dT_f}{dt} \\ \sigma_{SB}\varepsilon_{SA,f}T_b^4 + \dfrac{kA_{al}}{h}\left(T_f - T_b\right) + \sigma_{SB}\dfrac{\varepsilon_i(1-A_{al})}{2-\varepsilon_i}\left(T_f^4 - T_b^4\right) = C_{p,b}\dfrac{dT_b}{dt} \end{cases} \quad (4)$$

With,

$$Q_{SUN} = A_p\alpha_{SA}\cos\left(\alpha(t)\right)\frac{\phi_{1\,AU}}{D_s^2} \quad (5)$$

Here, $C_{p,f}$ and $C_{p,b}$ are the thermal capacity of the front and back surfaces respectively, A_p is the area of the single panel, α_{SA} is the absorptivity of the panel's front side, $\varepsilon_{SA,f}$ and $\varepsilon_{SA,b}$ are the emissivity of the panel's front and back sides, k is the conductivity of the aluminum honeycomb, $A_{al} = \rho_{hc}/\rho_{al}$ is the net aluminum cross section defined as the ratio between the density of the honeycomb and the density of the aluminum, h is the panel's thickness, ε_i is the emissivity of the internal surfaces (assumed equal to 0.6) and σ_{SB} is the Stephan Boltzmann constant. It has been considered also the power extracted from each panel read by the array power regulator Q_{APR} parameter, obtained from telemetry. The $\phi_{1\,AU}$ and D_s are respectively the energy solar flux at one astronomical unit from the Sun and the spacecraft actual distance from the Sun.

Model parameters were partly provided by the project $(k, h, A_p, \varepsilon_{SA,f}, \varepsilon_{SA,b}, \alpha_{SA})$ or estimated ($C_{P,f}, C_{P,b}, \alpha_{CTE}, A_{al}$) by matching the computed rear-side temperature with the corresponding measured data, collected in the same reference period. Fig. 7 shows the computed front-side temperature (red curve) and rear-side temperature (blue curve), obtained by solving (4, compared with the rear measured one (green curve). At this stage, (3 can be applied to compute the thermal snap acceleration induced by JUICE's solar array. To compare the modelled acceleration with the HAA measurements, the computed acceleration must be projected along the Acc0 sensitive axis and scaled by the ratio between the solar array mass and the total spacecraft mass $M_{SC} = 5700\ kg$. Additionally, the relative displacement between the spacecraft center of mass and the solar array center of mass must be considered. *Table 2* reports the values of parameters, either assumed or estimated, used to model the thermal behavior of JUICE solar arrays.

Parameter	Value
$C_{P,f}, C_{P,b}$	800 J/kg/K
A_{al}	$\frac{14\ kg/m^3}{2700\ kg/m^3}$
h	23 mm
k	117 W/m/k
$\varepsilon_{SA,f}, \varepsilon_{SA,b}$	0.82, 0.79
α_{SA}	0.80
ε_i	0.6
α_{CTE}	$3.5 \times 10^{-6}\ K/m$
A_p	8.8 m^2

Table 2 JUICE solar array properties

Fig. 8 shows the comparison between HAA Acc0 calibrated data after the removal of the Moon's gravity gradient signal and the computed thermal snap acceleration. This latter primarily occurred during the penumbra phase (yellow shadowed area), where the rapid transition from umbra condition (grey shadowed area) to the illuminated condition (white area), amplified both the thermal gradient and its second derivative. The computed quasi-static displacement of the solar array tip was estimated to be approximately 50 mm, corresponding to $\sim 0.3°$ of angular displacement. After the penumbra phase, HAA data shows a clear periodic signal easily explained by thermally induced vibrations of the solar array structure. This is confirmed by the amplitude spectral density (ASD) computed on HAA data after the spacecraft came back in full illumination (white area in Fig. 8), where we found that the dominant frequency closely matches the first out-of-plane mode of the solar array, as shown in Fig. 9. A similar phenomenon was observed at penumbra ingress; however, due to the slower transition from illumination to umbra, the perturbing signal was weaker, and the resulting displacement and corresponding acceleration detected by HAA were correspondingly smaller.

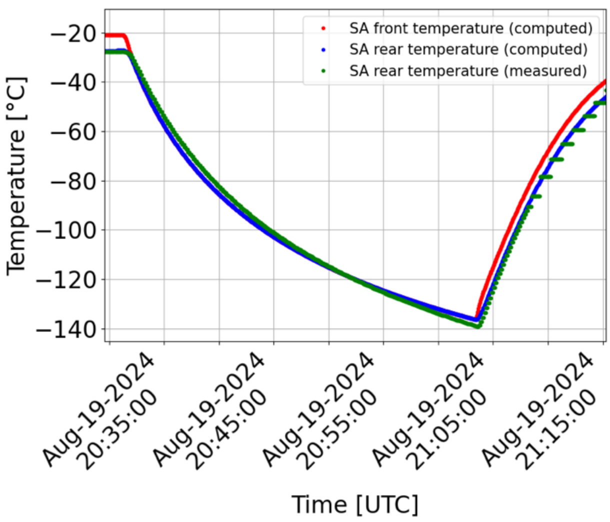

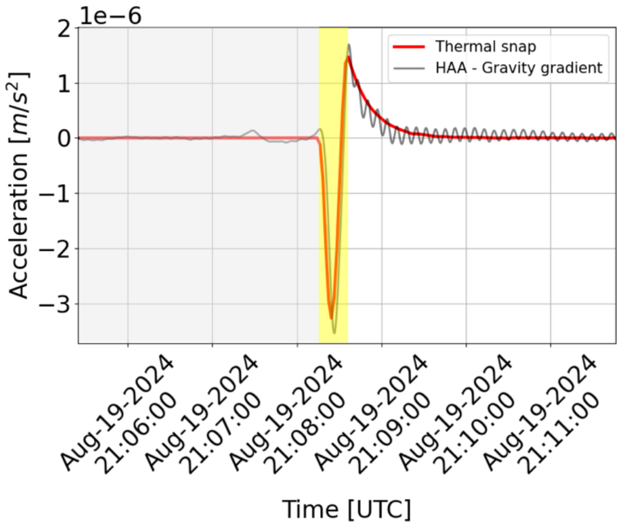

Fig. 7 Estimated solar array surface temperature on the front side (red) and rear side (blue), compared with measured rear-side temperature (green).

Fig. 8 HAA calibrated data collected during umbra exit (black curve) and computed thermal snap acceleration (red). Gray shadowed area: Eclipse phase; Yellow shadowed area: egress penumbra phase.

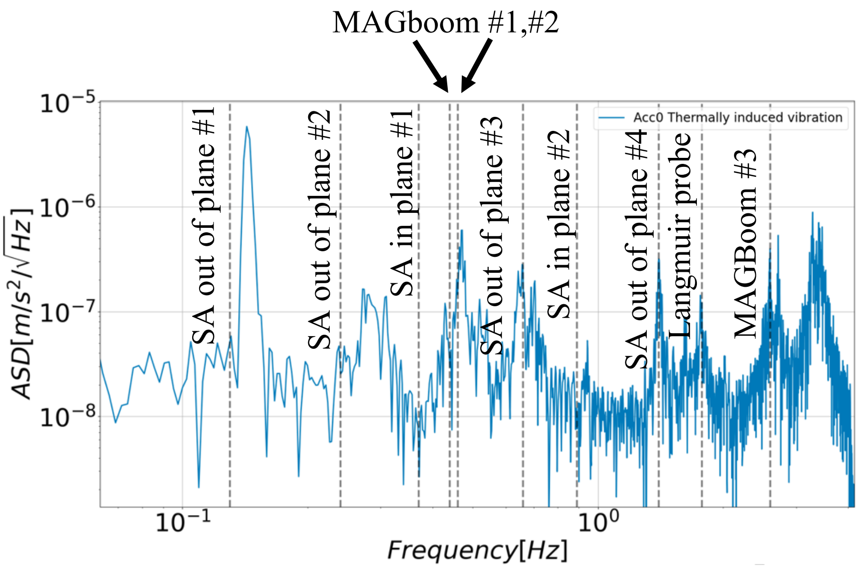

Fig. 9 ASD computed on HAA data soon after exit penumbra phase of Acc0 sensor. The vertical dashed lines indicate the proper modes of each appendages.

4.3 Unexpected signals

The great added value of an HAA onboard the spacecraft lies not only in its ability to directly measure expected accelerations that are difficult to model, but also in its capability to detect unforeseen accelerations which, if left uncalibrated, could degrade the performance of scientific experiments. During LEGA Moon flyby, HAA data revealed several unexpected signatures. These were already visible in previous pictures but left voluntarily uncommented. Fig. 10 puts evidence now on two similar signals about $\sim 10^{-4} m/s^2$ detected at 20:42 UTC and 21:26 UTC, highlighted within the red circles, while another significant acceleration of ~ $2 \cdot 10^{-6} m/s^2$ was detected shortly after the spacecraft crossed the lunar terminator (indicated by the blue dotted line and blue shaded area thereafter).

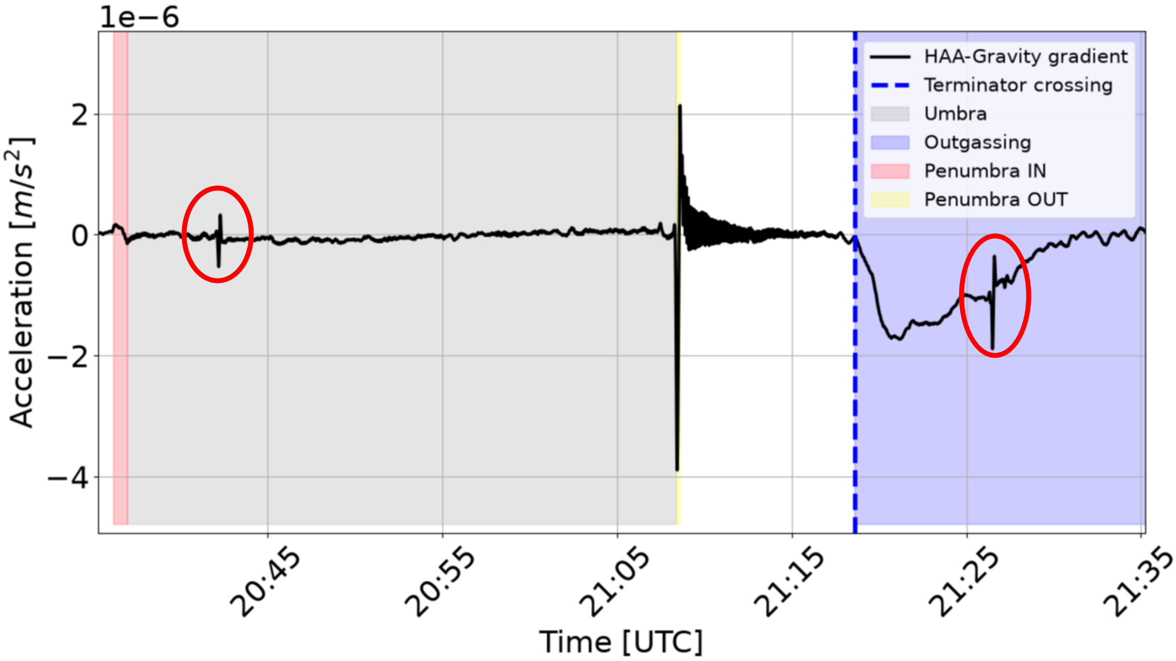

Fig. 10 HAA Acc0 calibrated data. Black curve: HAA calibrated data collected by Acc0 sensor subtracted for the Moon gravity gradient signal. Blue dotted line: Terminator crossing event; Red and yellow shadowed area: Ingress and egress penumbra phases; Gray shadowed area: Umbra phase; Blue shadowed area: Outgassing event region; Umbra phase Red circles: SWI telescope rotation signals

4.3.1 Submillimetre Wave Instrument operations

The first signal, identified by red circles in the Fig.10, appears to be associated with spacecraft activity related to the Submilimetre Wave Instrument (SWI), the only one featuring a steerable component and active at the corresponding epochs: a telescope mounted on the same spacecraft plate as the HAA (+X vault). Personal communication with the SWI instrument team confirmed that at 20:41:58 UTC the telescope was rotated by 72 degrees in the along-track direction to point toward the Moon (nadir position). A second rotation, in the opposite direction by 54 degrees, was performed at 21:27 UTC to observe the Moon in a backward-looking configuration. These mechanical operations primarily excited resonance modes of the spacecraft's MAGboom structure (0.44,0.46 and 2.6 Hz) and solar arrays (0.13, 0.21 and 0.89 Hz). The influence of these events on HAA data capability to support 3GM experiment has yet to be fully assessed. It is likely that dedicated tests will be required to thoroughly characterize possible interference issues.

4.3.2 Outgassing event

The second SWI event is superimposed to another clearly visible low-frequency phenomenon occurred onboard the JUICE spacecraft. After the eclipse event, JUICE reached the Moon CA at 21:14:50 UTC and soon after crossed the terminator at 21:18:35 UTC. Fig. 11 shows JUICE attitude during the terminator crossing. At that moment, the +Z and +X directions of JUICE were oriented toward the illuminated surface of the Moon, receiving most of the incoming heat due to lunar albedo and infrared radiation. One of the most plausible explanations for the effect is that the multilayer insulation (MLI) on the +Z vault may have accumulated frozen contaminants during the early cruise phase, as this surface is typically exposed to deep space. Given the combination of high incoming radiation and the low thermal inertia of the MLI, it is likely that its temperature increased rapidly, potentially triggering an outgassing event. A similar phenomenon was observed on the BepiColombo ESA–JAXA mission during a Venus swing-by, De Filippis et al., (2025).

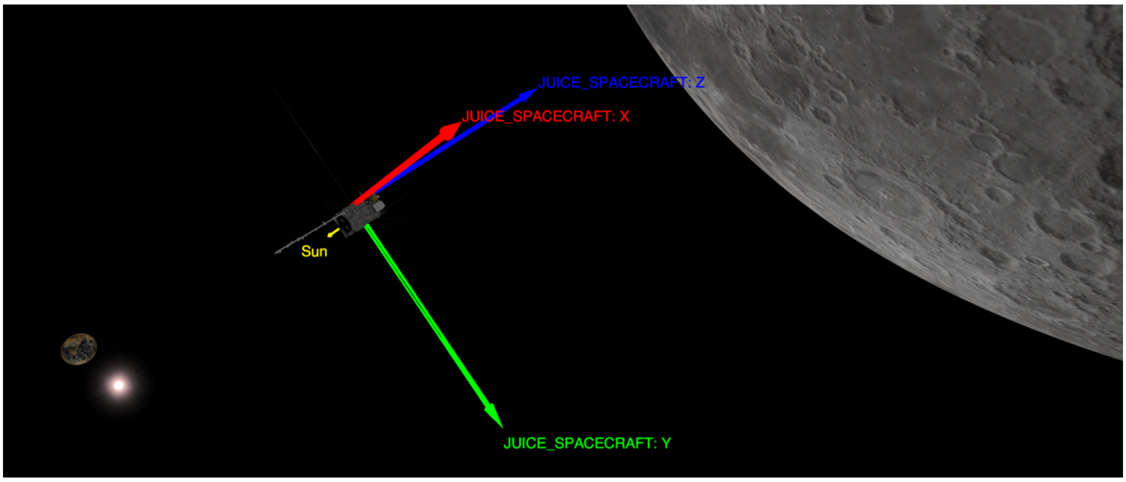

Fig. 11 JUICE attitude at terminator crossing (21:18 UTC) from Cosmographia

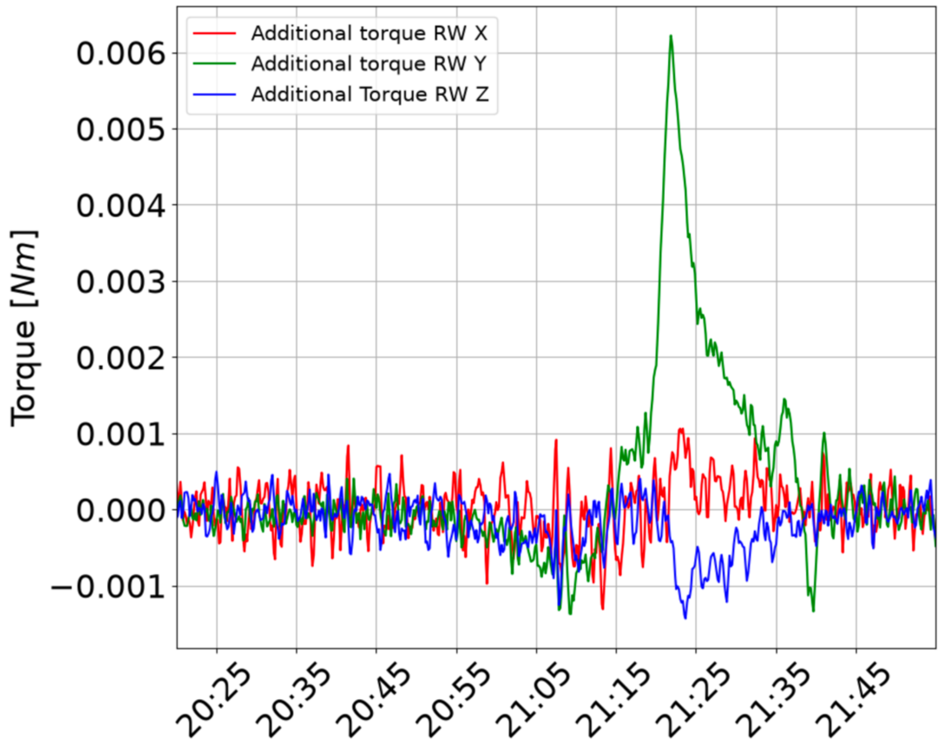

Fig. 12 Additional torques exerted by reaction wheels (RW) on the spacecraft along body fixed reference frame X (red), Y (green), Z (blue).

The JUICE spacecraft attitude and orbit control system (AOCS) also detected this event. Fig. 12 shows the unmodelled torque generated by the reaction wheels to maintain the commanded quasi-inertial attitude. The dominant torque component was observed along the +Y JUICE SPACECRAFT axis, while the main acceleration measured by HAA was along the -Z JUICE SPACECRAFT axis. Assuming that $M = M_{SC}\, r \times a$, where M is the unmodelled torque generated by the reaction wheels, r is the vector distance from the spacecraft center of mass and the outgassing location and a is the unmodelled acceleration measured by HAA, adopting the reasonable simplification that both torque and force acted predominantly along a single axis, the outgassing appears to have occurred approximately 50 cm from the spacecraft's center of mass, in the -X JUICE SPACECRAFT direction.

To further investigate the impact of the suspected outgassing event, we conducted an orbit determination analysis using Doppler data, collected during the Lunar gravity assist. The radiometric dataset consisted of X band two-way coherent Doppler data acquired by the ESTRACK ground stations at:

- New Norcia on 2024-08-19, from 11:09 UTC to 22:10 UTC, with an observed Doppler noise level of 0.035 mm/s @60s, and
- Cebreros, from 2024-08-19 22:26 UTC to 2024-08-20 04:15 UTC, with an observed Doppler noise level of 0.046 mm/s @60s.

Note that no 3GM's KaT operations were possible as it would have required a Ka band uplink signal, currently only available at Malargüe ground station. This analysis was performed with ESA's GODOT v1.11 software, using a setup adapted from radio science analyses, Cappuccio *et al.*, (2025). In a first attempt we tried to solve for ΔV_i components along all three spacecraft axes X, Y and Z, and the time event, but the reduced radiometric data set available for this analysis was not sufficient to fully decorrelate the three estimated impulses, resulting in a too large covariance matrix that was both consistent with estimates carried out by the Flight Dynamics (FD) team, Syndercombe et al. (2025) and null ΔV_i. The estimated time of the outgassing event was 2024-08-19 21:26 ± 42 seconds UTC. We had to accept to carry out a second constrained analysis in which ΔV_y was kept null and we obtained a better statistical compatibility with FD solution. In summary, the analysis based solely on radiometric data provides only limited constraints on the characteristics of the outgassing event, which is detected with significantly greater sensitivity by the accelerometer measurements. Consequently, the HAA data were not included in the orbit determination process because it would not produce any significant effect on the orbital solution.

Indeed, along the +Z direction, HAA measurements are consistent with a $\Delta V_y = -0.7\ mm/s$. Integrating a different portion of HAA data where no signals were detected, we associated to the outgassing impulse a maximum error of 0.1 mm/s. Along the +X direction, HAA measurements are strongly affected by the thermal disturbances, making the collected data unreliable. However, an upper bound for the ΔV_x and ΔV_y can be defined from the formal uncertainty of the orbit determination process. Considering 3σ formal uncertainties, an upper bound for the other components of the outgassing induced ΔV can be provided, $|\Delta V_x| \leq\ 0.3\ mm/s$ and $|\Delta V_y\ | \leq\ 5.4\ mm/s$.

After the outgassing, the spacecraft's momentum changed according to the push exerted by sublimated products. Using the conservation of momentum, the sublimated product's effective exit velocity V_{sub} and its mass m_{sub} can be related to the overall change in the spacecraft's velocity DV:

$$m_{sub}V_{sub} = M_{SC}DV \qquad (6)$$

The most plausible outgassing product is water ice, as also suggested by observations from different instrument teams during the flyby. Under this assumption, we can follow the same analysis made by Sandford *et al.*,(2020), to estimate the mass of the outgassed products.

The effective exit velocity of the sublimated water vapor can be estimated by considering the theoretical maximum velocity for a sublimating gas, given by Bird et al. (2002):

$$V_{lim} = \sqrt{\frac{2\gamma RT}{\gamma - 1}} \qquad (7)$$

where γ is the ratio of specific heat of water, $R = 461.5 \text{ J/kg/K}$ is the specific gas constant, and T is the total temperature at zero velocity. For typical value of $\gamma = 1.33$ and $T = 300K$, the $V_{lim} = 1000\ m/s,$ However, this is only a physical maximum value, and the true value of the effective exit velocity is not easy to retrieve. Considering that the actual exit velocity V_{sub} can be up to $V_{sub} = 1/2V_{lim} = 500\ m/s$, it's possible to give an estimate of the upper limit for the sublimated product's mass:

$$m_{sub} = M_{SC}DV/V_{sub} = 8g \qquad (8)$$

Note that the true value of the effective exit velocity may differ in relation to the sublimation dynamics. If $V_{sub} = V_{lim} = 1000\ m/s$, the outgassed mass became $m_{sub} = 4\ g$. Hence, is possible to assess that the sublimated products mass could be estimated within the range of [4-8] gr.

Moreover, the estimation of sublimated particles along the other spacecraft axes is even more challenging. However, the accelerometer data provided indication that the outgassing components along those directions are significantly smaller than along the +Z JUICE SPACECRAFT axis.

5 Conclusions

This work presents a comprehensive analysis of data collected by the High Accuracy Accelerometer instrument during the JUICE LEGA flyby at the Moon. The calibrated scientific dataset was compared with predicted non-gravitational signals derived from analytical models, showing good agreement between the HAA Acc0 sensor measurements and the expected reference signals. In details, the HAA on board JUICE detected the effect of the Moon gravity gradient on its proof masses as well as thermoelastic displacement and periodic oscillations of solar array during the penumbra phases. In addition, unexpected dynamical effects on the spacecraft have been detected. The operations activities of the Submillimetre Wave Instrument (SWI) were clearly visible in the HAA data. The rotation of the instrument's steerable telescope, performed before and after the Moon closest approach to achieve nadir pointing, excited structural resonance modes of the spacecraft, notably the MAGboom and solar array. The resulting vibrations were observed on all three HAA axes. The assessment of the impact of these effects on HAA science data is out of the scope of this paper and dedicated analysis will be performed in the future. Later on, an outgassing event occurred soon after the spacecraft transition over the Moon terminator was detected by the instrument Acc0 channel. The source of the signal was also confirmed by multi-instrument analysis and spacecraft AOCS telemetry. The measured accelerations profile suggested that the outgassing happened mostly along spacecraft -Z direction producing a total $\Delta V = 0.7\ mm/s$ along the same direction. The estimated order of magnitude for the mass of sublimated water ice product was in the range between 4g and 8g. These observations provided important information for the instrument calibration and spacecraft dynamic environment during close flyby. Moreover, HAA's proven ability to detect such accelerations is particularly important in the context of the 3GM radio science experiment. Indeed, these unexpected accelerations, which are challenging to model accurately, may compromise the quality of the scientific results if they are not adequately considered during orbit determination.

The acquisition of HAA in-flight data prior the start of the scientific phase will be fundamental to achieve optimal instrument performance. It will enable the definition of the most suitable instrument configuration parameters, enhance the reliability of subsequent measurements, and support the development of improved operational strategies. Early data will help optimize the coordination with other onboard instruments, thereby maximizing the overall scientific return of the mission.

6 Data availability

HAA data set used in this publication is available in the ESA Planetary Science Archive (PSA) Guest Storage Facility (GSF), European Space Agency (2026).

7 Author contribution

UDF,PC,MDB wrote the manuscript draft; UDF,MDB,LI planned the operations; UDF,PC analyzed the data; UDF,PC,MDB,IDS,DD,LI reviewed and edited the manuscript.

8 Competing interests

The authors declare that they have no conflict of interest.

9 Acknowledgments

The authors are grateful to the Italian Space Agency (ASI) for financial support through ASI-INAF Agreement No. 2023-6-HH.0 in the context of ESA's JUICE mission.

10 References

Benkhoff J. et al., “BepiColombo - Mission Overview and Science Goals,” *Space Sci Rev*, vol. 217, no. 8, p. 90, 2021, doi: 10.1007/s11214-021-00861-4.

Bird R. B., “Transport phenomena,” *Appl. Mech. Rev.*, vol. 55, no. 1, pp. R1–R4, Jan. 2002, doi: 10.1115/1.1424298.

Cappuccio P. and G. Cascioli, *ESA’s JUICE End-to-End Orbit Determination Simulation to Calibrate On-Board Accelerometer*, 2018.

Cappuccio P., M. Di Benedetto, G. Cascioli, and L. Iess, “Report on JUICE 3GM gravity experiment performance,” in *European Planetary Science Congress*, 2018, pp. EPSC2018-1066.

Cappuccio P. et al., “Report on First Inflight Data of BepiColombo’s Mercury Orbiter Radio Science Experiment,” *IEEE Trans Aerosp Electron Syst*, vol. 56, no. 6, pp. 4984–4988, Dec. 2020, doi: 10.1109/TAES.2020.3008577.

Cappuccio P. et al., “Ganymede’s gravity, tides and rotational state from JUICE’s 3GM experiment simulation,” *Planet Space Sci*, vol. 187, p. 104902, 2020, doi: https://doi.org/10.1016/j.pss.2020.104902.

Cappuccio P., M. Di Benedetto, D. Durante, and L. Iess, “Callisto and Europa Gravity Measurements from JUICE 3GM Experiment Simulation,” *Planet Sci J*, vol. 3, no. 8, p. 199, Aug. 2022, doi: 10.3847/PSJ/ac83c4.

Cappuccio P. et al., “Analysis of Radio Science Data from the KaT Instrument of the 3GM Experiment During JUICE’s Early Cruise Phase,” *Aerospace*, vol. 12, no. 1, p. 56, Jan. 2025, doi: 10.3390/aerospace12010056.

De Filippis U. et al., “Pseudo-Drag-Free System Simulation for Bepicolombo Radio Science Using Accelerometer Data,” *Journal of Guidance, Control, and Dynamics*, vol. 47, no. 4, pp. 685–696, Jan. 2024, doi: 10.2514/1.G007916.

De Filippis U. et al., “Monitoring JUICE deployment operations with high-accuracy accelerometer data,” *Acta Astronaut*, vol. 225, pp. 719–728, Dec. 2024, doi: 10.1016/j.actaastro.2024.09.047.

De Filippis U., C. Lefevre, M. Lucente, C. Magnafico, and F. Santoli, “Characterization of the outgassing event during BepiColombo second Venus flyby using Italian Spring Accelerometer data,” *Acta Astronaut.*, vol. 226, pp. 11–19, Jan. 2025, doi: 10.1016/j.actaastro.2024.09.062.

De Marchi F., P. Cappuccio, G. Mitri, and L. Iess, “Frequency-dependent Ganymede’s tidal Love number k2 detection by JUICE’s 3GM experiment and implications for the subsurface ocean thickness,” *Icarus*, vol. 386, p. 115150, 2022, doi: https://doi.org/10.1016/j.icarus.2022.115150.

Del Vecchio E. et al., “First Analysis of BepiColombo Radio Science and Accelerometer Data Acquired During Venus and Mercury Flybys,” *IEEE Trans Aerosp Electron Syst*, vol. 60, no. 4, pp. 5604–5612, Aug. 2024, doi: 10.1109/TAES.2024.3381582.
di Stefano I., P. Cappuccio, M. Di Benedetto, and L. Iess, “A test of general relativity with ESA’s JUICE mission,” *Advances in Space Research*, vol. 70, no. 3, pp. 854–862, Aug. 2022, doi: 10.1016/j.asr.2022.05.005.

European Space Agency, *ESA-JUICE_LEGA-Special-Issue_v1.0*, 2026, doi: https://doi.org/10.57780/esa-2bb387d.

Grasset O. et al., “JUpiter ICy moons Explorer (JUICE): An ESA mission to orbit Ganymede and to characterise the Jupiter system,” *Planet Space Sci*, vol. 78, pp. 1–21, 2013, doi: https://doi.org/10.1016/j.pss.2012.12.002.

Grasset O., D. Titov, and O. Witasse, “Jupiter Icy Moon Explorer Mission,” in *Encyclopedia of Astrobiology*, M. Gargaud, W. M. Irvine, R. Amils, P. Claeys, H. J. Cleaves, M. Gerin, D. Rouan, T. Spohn, S. Tirard, and M. Viso, Eds., Berlin, Heidelberg: Springer Berlin Heidelberg, 2023, pp. 1587–1591, doi: 10.1007/978-3-662-65093-6_5283.

Johnston D. J. and E. A. Thornton, “Thermally Induced Dynamics of Satellite Solar Panels,” *J Spacecr Rockets*, vol. 37, no. 5, pp. 604–613, Sep. 2000, doi: 10.2514/2.3633.

Lopez A. E., R. Valles, R. Andres, and C. Arviset, “An Update on SPICE for ESA Missions,” *Bulletin of the AAS*, vol. 55, no. 8, 2023. https://baas.aas.org/pub/2023n8i109p08

Magnafico C. et al., “Italian Spring Accelerometer measurements of unexpected Non Gravitational Perturbation during BepiColombo second Venus swing-by,” *Acta Astronaut.*, vol. 232, pp. 14–22, Jul. 2025, doi: 10.1016/j.actaastro.2025.02.037.

Sandford S. A. et al., “Outgassing from the OSIRIS-REx sample return capsule: characterization and mitigation,” *Acta Astronaut.*, vol. 166, pp. 391–399, Jan. 2020, doi: 10.1016/j.actaastro.2019.07.043.

Santoli F. et al., “ISA, a High Sensitivity Accelerometer in the Interplanetary Space,” *Space Sci Rev*, vol. 216, no. 8, p. 145, 2020, doi: 10.1007/s11214-020-00768-6.

Shapira A. et al., “An Ultra Stable Oscillator for the 3GM experiment of the JUICE mission,” in *2016 European Frequency and Time Forum (EFTF)*, IEEE, Apr. 2016, pp. 1–5, doi: 10.1109/EFTF.2016.7477766.

Syndercombe T., F. Budnik, and R. Meles, “The JUICE navigation campaign for the first combined Lunar-Earth gravity assist,” in *18th International Conference on Space Operations*, Montreal: SpaceOps-2025, May 2025.

Van der Ha J. and S. D., “Thermal Radiation Effects on Deep-Space Trajectories,” *Advances in the Astronautical Sciences*, vol. 136, pp. 1861–1880, Jan. 2010.